International Journal of
Science Inventions Today
www.ijsit.com
ISSN 2319-5436
Research Article

STUDY OF NANOSECOND ND: YAG 213 nm LASER ABLATION OF EXTRA HEAVY CRUDE OIL BY INDUCTIVELY COUPLED PLASMA MASS SPECTROMETRY

Henry Wuyke*[1], Llinaber Feo[1] and Miguel Murillo[2]

*[1]*PDVSA-INTEVEP S.A. Urbanización Santa Rosa. Sector El Tambor. Los Teques. Estado Miranda. Apdo. 76343, Caracas 1070A, Venezuela*

[2]Centro de Química Analítica, Facultad de Ciencias, Universidad Central de Venezuela, Apdo. 47102, Caracas 1070A, Venezuela.

ABSTRACT

The Laser-Extra Heavy Crude Oil interaction was studied using a nanosecond Nd:YAG 213 nm laser coupled to an ICP-MS. For this study, ~2.7 g Extra Heavy Crude Oil was mixed with ~3 mL xylene and 0,3 g organic multielemental solution containing 100 µg g^{-1} of Ag, Al, Ba, Cd, Cr, Cu, Mg, Mn, Mo, Ni, Pb, Sn, Ti, V, and Zn, xylene was left to evaporate at 90 °C and multielemental samples were obtained and analyzed by LA-ICP-MS. Laser parameters, such as, ablation gas flow, sample scanning speed, spot size, fluence and focus position were optimized and RSD (n = 8) from 3% to 5% for the net signal of ^{63}Cu, ^{95}Mo, ^{60}Ni and ^{66}Zn and from 0.9% to 3.3% for the ratios Ni/Mo and Cu/Zn were obtained. Elemental fractionation was observed with both Zn and Cd when fluence was varied. Nevertheless, evidence is not enough to explain results as a consequence of high volatility or high ionization potential (PI) of these elements. Ablation craters obtained show signs of more pronounced thermal processes at higher fluences. Elemental fractionation was also observed in the ICP due to mass load effect. Isotopic ratios $^{95}Mo/^{112}Cd$, $^{63}Cu/^{66}Zn$ y $^{27}Al/^{24}Mg$, which have different ionization potential (1.89; 1.68 and 1.66 eV, respectively expressed as $PI_{denominator}$ - $PI_{numerator}$) increase when mass load is increase. On the other hand, $^{60}Ni/^{63}Cu$ ratio (0.09 eV difference) remains constant. These results indicate that the plasma ionization temperature decreases when mass load is increased affecting those elements with high ionization potential.

Keywords: Laser Ablation, ICP-MS, Extra Heavy Crude Oil, Elemental Fractionation

INTRODUCTION

The use of LA-ICP-MS to analyze crude oil may be advantageous to eliminate the extensive sample treatment steps of traditional methods such as calcination or acid digestion. However, few works using LA-ICP-MS for direct elemental analysis in crude oil have been reported [1-3]. It can be probably due to difficulties found during ablation, such as splashing, of this type of liquid samples. LA-ICP-MS is more suitable for solid samples [4-7]. Therefore, it is a potential tool for direct analysis of semi-solid extra heavy crude oil with less trouble in the ablation process.

The ablation process is strongly dependent on the properties of the sample such as composition, thermal diffusivity and absorptivity [4]. Therefore, matrix matched calibration standards or reference certificated materials are required to ensure accuracy of results. However, calibration standards are not available for the majority of sample matrixes, which limits the applications of LA-ICP-MS [8,9]. Therefore, it is important to know how the laser ablation of extra heavy crude oil is affected by each experimental parameter and identify which of them lead rise to fractionation or non-stoichiometric sampling.

Pulse length is one of the most important parameters involved in mechanisms by which the ablation laser process occurs. Lasers with pulse length in nanosecond (ns) and femtosecond (fs) are the most frequently used in LA-ICP-MS applications. Generally, fs lasers produce better results because the time interval of energy delivering is much smaller than the time interval needed for the thermal stabilization of the sample (in the order of picoseconds) [6,10]. Furthermore, photon intensities reach values of $> 10^{14}$ W cm^{-2}, thereby processes are predominantly non-thermal, causing less collateral damage, less dependence on the matrix, smaller particles and non laser-plasma interaction [6]. Nevertheless, even though the latest developments are aimed to take advantage of fs lasers, today ns lasers are still very popular due primarily to their low cost.

Fluence also plays an important role in ablation mechanisms. It must be above a threshold value to lead the ablation process [10]. When ns lasers are used, fluence should not be too high to avoid the generation of a high electron density plasma, because it increases the laser-plasma interaction and therefore, reduces the interaction between the laser and the sample [11]. When fs lasers are used, fractionation appears to be only near the threshold value of the sample and reach an asymptotic value as the fluence increases [9,12-14].

Fractionation according to the fluence in the range of 2 to 42 J cm^{-2} with a fs laser in brass, aluminum and glass samples was assessed by Bian et al. [12]. In those conditions, the ratio Zn/Cu in the brass and aluminum samples was independent of the fluence while for glass samples there was a strong dependency especially for the most transparent glass sample (NIST 610). However, at higher fluence, the ratio Zn/Cu reached an expected asymptotic value, considering the results of brass and aluminum measures. Similar results on the same glass sample type were obtained by Koch et al. [13]. Fractionation was observed with

ratios Zn/Cu and Mo/Ni which have different ionization potentials but not with the ratio U/Th which have similar ionization potentials (PI: U: 6.2 eV, Th: 6.3 eV y Pb: 7.5 eV), which evidence of that the ionization potential affects the ablation process. It has been mentioned that Coulomb interactions are responsible for this behavior [11]. However, ablation mechanisms are still not fully understood to the date [15]. There are other factors such as the volatility of the elements that influence the signals when thermal processes occurred, *i.e.* more volatile elements are vaporized preferentially, resulting in greater signal and causing fractionation [12,16].

Fractionation has also been studied as a function of time, *i.e.* shot to shot. Garcia et al. [9] studied this effect using a fs laser in binary metallic, semiconductors and glasses samples. They obtained that the Cu/Zn changes from shot to shot reached an asymptotic value independent of fluence, which corresponds to a stoichiometric sampling. Furthermore, this asymptotic value is reached faster if high fluence is applied.

There are other parameters that also affect the ablation process such as ablation gas and laser wavelength. Helium and argon are the most used gases for ablation environmental and sample transportation. However, as argon has a lower ionization potential than helium, there is a greater likelihood of plasma formation and shielding effect that prevent an efficient interaction between laser and sample, so that helium is preferred [11]. Wälle et al. [17] using ns and fs lasers in glass, zircon and silicon samples, observed a depression of the detection efficiency by a factor of 5 when used argon instead of helium as ablation gas. Studies have shown that using shorter wavelengths, with both ns and fs lasers in glass samples fractionation effects are reduced [13,18,19].

Particles generated in the ablation process can have different compositions in terms of size, especially if a ns laser is used [6]. It creates fractionation if there is no transport efficiency, because large particles (> 1 μm) tend to be lost by gravity or deposited on chamber ablation. While, small particles (<10 nm) are lost by diffusion or electrostatic effects [12]. The ideal condition is that all particles are fully decomposed when reaching the ICP in order to to avoid affecting the characteristics of plasma. Nevertheless, it has been found that mass load that reaches the ICP can create a matrix effect dependent on the ionization potential [13] or on the melting point of the elements [20].

Although LA-ICP-MS has been used for elemental analysis in crude oil [1,3] a systematic study that assess the fractionation of these types of samples, as is usually done on metal alloys or glass samples, has not been performed. The aim of this study is to evaluate the behavior of laser - extra heavy crude oil interaction by LA-ICP-MS as a function of various experimental parameters using a ns Nd: YAG laser at 213nm.

MATERIALS AND METHODS

Instrumentation:

Laser ablation was performed using a Nd:YAG UP-213 LA New Wave Research operated at 213 nm with a pulsed duration of ~ 4 ns. An ICP-MS Agilent Technologies 7500ce that consist in a plasma source, a octopole reaction cell and a quadrupole mass analyzer was used. Laser ablation and ICP-MS were connected using Tygon tubes (S-50-HL Class VI, ~ 3 mm i.d.) as shown in Fig. 1. In analysis, the aerosol from the ablation cell is mixed with Ar using a "Y" connection, then goes to a cyclone chamber of ~ 4 cm diameter and finally to the ICP-MS. The bypass and purge valves are used for analysis preconditioning.

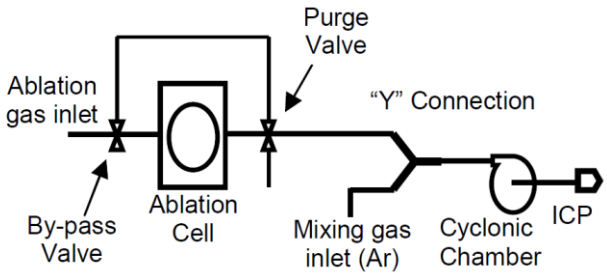

Figure 1: Coupling laser ablation to ICP-MS

Reagents, stardards and samples:

Extra heavy crude oil samples (API° < 10) were provided by PDVSA-INTEVEP. Xylene (puriss. p.a.) Sigma-Aldrich and an organic multielemental solution containing 100 μg g^{-1} of Ag, Al, Ba, Cd, Cr, Cu, Mg, Mn, Mo, Ni, Pb, Sn, Ti, V and Zn, S-21 Conostan, USA were used. The tuning solution to perform the ICP-MS was prepared from ARM™ Absolute Standards, INC.1000 mg/Kg of Li, Mg, Co, Y, Ce and Pb in 2% HNO_3.

Sample preparation:

Approximately 2.7 g of oil was dissolved in a beaker with 2 mL xylene and 0.3 g of organic multielemental solution, the mix was homogenized by magnetic stirring and brought to an oven at 90 ° C for 2 hours until evaporation of xylene. Finally, part of the oil was placed in a sample holder tray of 1 cm diameter and 3 mm high and led to LA-ICP-MS. The resulting mixture contained a concentration of 10 μg g^{-1} in metals from the organic multielemental solution.

General conditions of analysis:

In this work, several experiments were performed in order to study the laser - extra heavy crude oil interaction by ICP-MS. Table 1 shows the general conditions of analysis. Isotopes of each element were

chosen to minimize isobaric and polyatomic interferences.

The ICP-MS parameters were those that resulted in good sensitivity for all elements of the tuning solution, covering a wide tuning range of masses: ^{7}Li, ^{24}Mg, ^{59}Co, ^{89}Y, ^{140}Ce and ^{208}Pb. Once sample is introduced into the ablation cell, the system is purged with He 1 L min^{-1} flow for 5 min.

ICP-MS	**Agilent 7500ce**
Plasma gas flow, L min^{-1}	15
Foward power, W	1500
Sample depth, mm	6.5
Integration time per point, s	0.1
Integration time per mass, s	0.3 (3 point per mass)
Laser ablation	**New Wave Research UP-213 LA**
Ablation gas flow (He), L min^{-1}	0.75
Mixing gas flow (Ar), L min^{-1}	0.5
Fluence, J cm^{-2}	~ 34 (100 %)
Focus, mm	4 (above the sample)
Spot size, µm	100 (1000 µm to 4 mm of defocus)
Pulse frequency, Hz	20
Scanning speed, µm s^{-1} (linear)	20

Table 1: General conditions of analysis

RESULTS AND DISCUSSION

A typical ablation profile of Ni, Cu, Zn and Mo is shown in Fig. 2. It is observed that the signal of Ni is much greater than the signals of Cu, Zn and Mo. This is because Ni is one of the major elements in the crude oil. However, there is good signal stability for the four elements at different concentration levels. Therefore, Cu and / or Zn signals were used to shown the optimization of the laser parameters and were selected for their differences in ionization potential (PI) and melting point (mp) (PI/mp: Cu 7.72 eV / 1083 °C, Zn 9.42 eV / 419 °C).

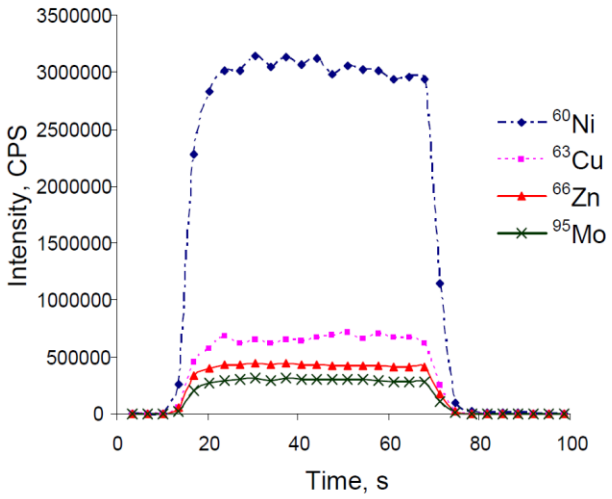

Figure 2: Ablation profile of ^{60}Ni, ^{63}Cu, ^{66}Zn and ^{95}Mo at general analysis conditions. Ablation time was 50 s with 10 s of delay relative to the acquisition start

Optimization of the laser parameters was performed with the aim of achieving the greatest intensity for ^{60}Ni, ^{63}Cu, ^{66}Zn and ^{95}Mo isotopes while maintaining good repeatability. In experiments with He-Ar as ablation gas and mixing gas respectively, flow rates were optimized between 0.4 – 0.9 L min^{-1} and the best results were obtained with 0.75 L min^{-1} He and 0.5 L min^{-1} Ar. In the Ar-Ar system, flow rates were optimized between 0 to 1.2 L / min, and the best results were obtained with 1.0 L min^{-1} Ar (ablation gas) and 0.2 L min^{-1} Ar (mixing gas).

Both He and Ar as ablation gases were compared in terms of the transient signal produced. The results are shown in Fig. 3. Figures 3a and 3c show that ^{63}Cu and ^{66}Zn signals are greater when He is used as ablation gas. Furthermore, a more pronounced memory effect is observed when Ar is used as ablation gas (figures 3b and 3d).

The damage on crude oil surface is greater when Ar is used in the ablation cell (figure 4) at both optimum analysis conditions (4 mm of defocus) and focus. These results are consistent with previous studies [11,17], where it is argued that Ar, which posses an ionization potential (15.7 eV) lower than He (24.6 eV), promotes the formation of plasma on the surface, which interacts with the sample and deform it, *i.e.* there are significant thermal processes.

The memory effect produced when Ar is used can be explained by the expansion to large volume of the ablated material into the ablation cell. It makes that the system takes longer to transport this volume. It has been mentioned that this expansion is more pronounced when the ionization potential is decreased [11]. It agrees with the results obtained in this study.

He was chosen as ablation gas for the subsequent experiments because it produces a significantly high signal for Cu, Zn, Ni and Mo (Student t test with $\alpha = 0.05$) and an improved precision to the Cu/Zn and Ni/Mo ratios (Fisher F test $\alpha = 0.05$) when compared to the obtained with Ar as ablation gas. Results are shown in table 2.

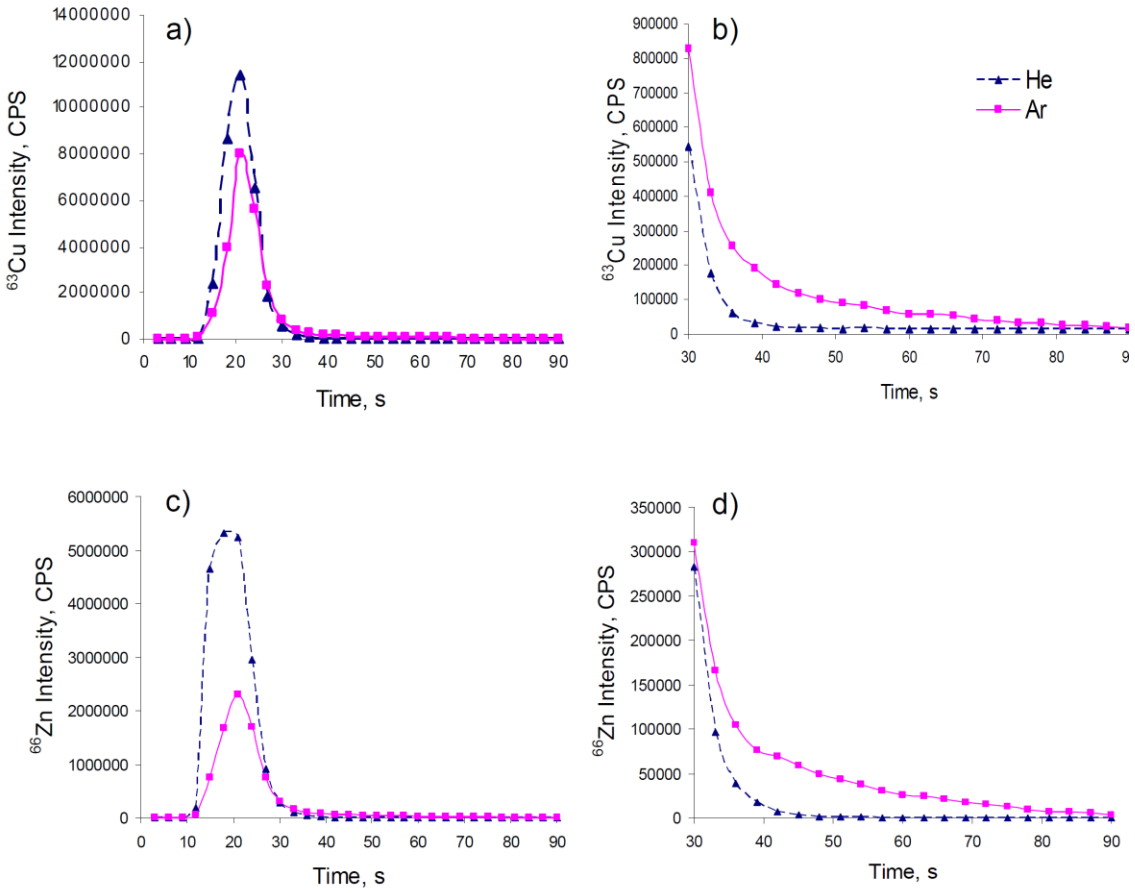

Figure 3: Signal versus time for two ablation gases, He and Ar: a and b) CPS of ^{63}Cu, c and d) CPS of ^{66}Zn. a and c) approximately at 10 s, the laser was switched on 7s (140 pulses), b and d) zoom between times 30 and 90 s

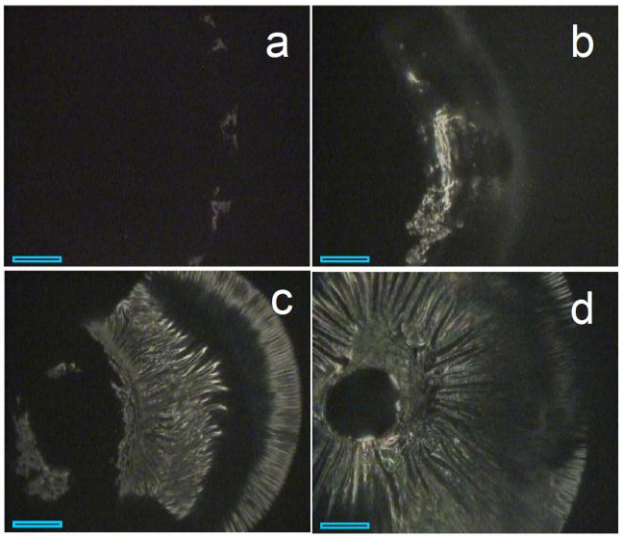

Figure 4: Pictures of craters at different ablation conditions. It is indicated in order: ablation gas, pulses number and defocus level (mm): a) He, 1000 pulses, 4 mm, b) Ar, 1000 pulses, 4 mm, c) He, 400 pulses, 0 mm (in focus), d) Ar, 100 pulses, 0 mm (in focus). The mark corresponds to 100 μm. He and Ar flow in the ablation cell were 0.75 L min^{-1}

Element o ratio	Signal Average (CPS). He	SD (CPS). He	CV (%). He	Signal Average (CPS). Ar	SD (CPS). Ar	CV (%). Ar
Cu	8.1E5	0.3E5	3.7	4.6E5	0.3E5	6.5
Zn	4.6E5	0.2E5	4.3	2.0E5	0.1E5	5.0
Ni	4.2E6	0.1E6	2.4	2.4E6	0.2E6	8.3
Mo	6.1E5	0.2E5	3.3	3.5E5	0.3E5	8.6
Cu/Zn	1.754	0.058	3.3	2.15	0.12	5.6
Ni/Mo	6.990	0.061	0.9	6.99	0.22	3.1

Table 2: Media, standard deviation (SD), coefficient of variation (CV) and sample size (n) for Cu, Zn, Ni and Mo signals and Cu/Zn and Ni/Mo ratios using He or Ar as ablation gas

The effect of two cyclone chambers with different sizes (~ 4 cm and ~6 cm internal diameter) was evaluated. Figure 5 shows that per run, the signal is more stable when a cyclone chamber is used, because it seems to dampen the effect produced in the ablation cell. Among ~ 4 cm and ~ 6 cm chambers no great differences were obtained. Therefore, ~ 4 cm chamber was taken as condition routine to make smaller the volume of the transport region.

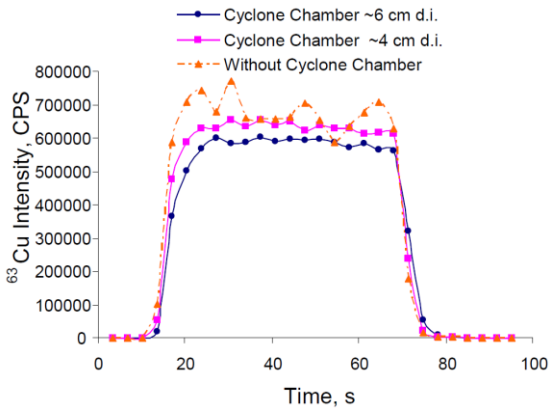

Figure 5: ^{63}Cu signal versus time with two cyclone chambers and without them. Ablation time was 50 s with 10 s of delay with 10 s delay relative to the acquisition start

In most of the works reported on solid samples, it is preferred ablate with a scanning speed different to zero, because at the same point, it begins to form an increasingly deep crater with each impact of the laser. The efficiency of energy transfer from the laser to the sample is continuously decreased and fractionation is observed. With a scanning speed different to zero, ablation is carried out over a greater area, which ensures a stoichiometric sampling.

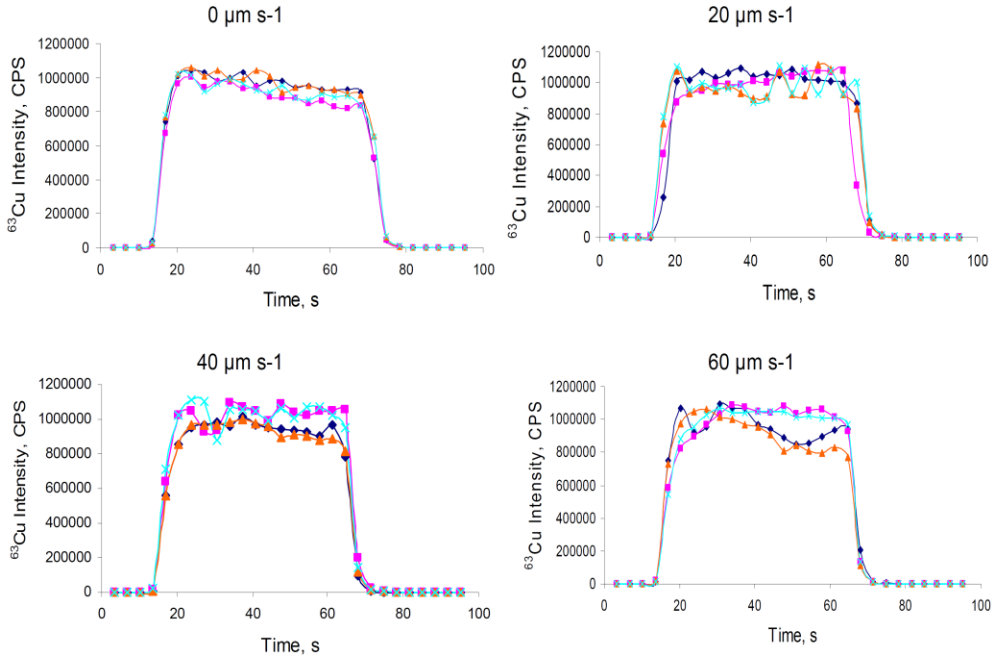

Figure 6: ^{63}Cu signal versus time for the four scanning speeds indicated. Four replicates are shown. Ablation time was 50 s with 10 s of delay relative to the acquisition start

Four linear scanning speeds 0, 20, 40 and 60 μm s^{-1} were tested in this work. Fig. 6 shows the ablation profiles of the four scanning speeds with four repetitions each one. At 0 μm s^{-1} reproducible profiles with a signal drop from the beginning to the end of the run between 10 and 15% are observed. However, Fig. 7 shows that there is no fractionation of $^{63}Cu/^{66}Zn$ ratio at 0 μm s^{-1}. Profiles at speeds 20 and 40 μm s^{-1} are little less stable and reproducible than at 0 μm s^{-1}, but without signal drop. The profile at 60 μm s^{-1} is more random probably for the larger sample area covering, which is not on the same horizontal axis (the crude oil sample on holder may be concave or convex and it is not easy to reproduce a flat surface). Besides from the beginning to the end of the run, its vertical position has changed, varying the level of defocus and so the sensitivity. Even though, the $^{63}Cu/^{66}Zn$ ratio remained stable through time at four scanning speeds studied (see Fig. 7). Finally, it can be established that the most appropriate conditions for the analysis are at small scanning speeds ~ 20 μm s^{-1}.

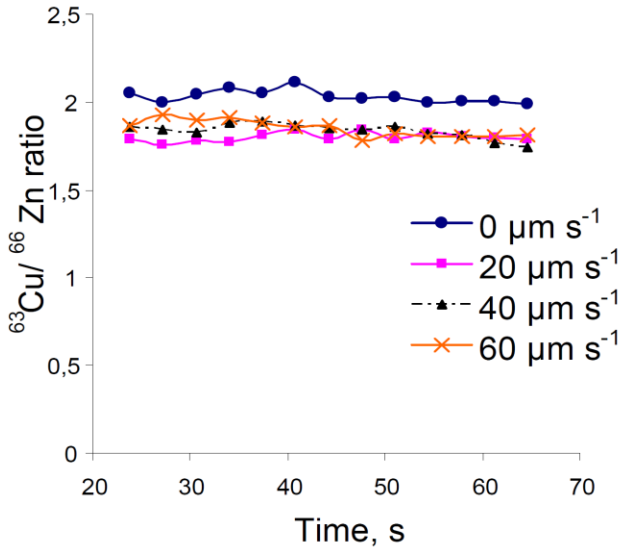

Figure 7: $^{63}Cu/^{66}Zn$ ratio versus time at four scanning speeds. Signals were recorded in the same experiment of Fig. 6

The fractionation effect versus fluence was evaluated with 15 elements by varying of defucus level which allows to work in a greater range instead of varying the energy to a fixed diameter. As can be seen in Fig. 8, the greater signal was obtained at higher positive defocus levels. Although fluence becomes smaller, it is still sufficient to ablate a larger area the crude oil sample, which explains the results.

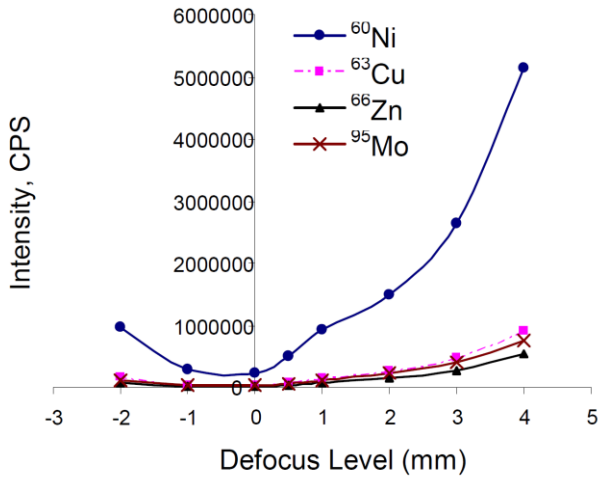

Figure 8: ^{60}Ni, ^{63}Cu, ^{66}Zn and ^{95}Mo signals versus defocus level. Each point represents the average of three 30 s runs of signal acquisition

Figure 9 shows the relationship between the elements studied and ^{66}Zn (Zn was chosen for its high ionization potential and high volatility) versus fluence. In general, fractionation was observed, *i.e.* M/^{66}Zn ratio increases with increasing fluence, except for Cd that appears to be stable, since it has very similar characteristics to Zn. Zn and Cd that present this fractionation with respect to the other elements, have high ionization potential and high volatility.

The observed behavior is hard to explain because ablation mechanisms are not yet fully known at the date [15]. However, trends indicate that when the ablation is carried out by thermal processes, more volatile elements are preferentially volatilized [6]. Recent results[13] suggest that elements with low ionization potential are preferentially ableated and coulomb interactions are responsible of that [11].

The results shown in Fig. 9 indicate that at lower fluences, Zn signal is favored compared to the other elements (except for Cd), contrary effect to that observed in previous studies on glass samples [12,13]. The results can not be explained by volatility if it is considered that there are greater thermal processes at high fluences or at least greater surface damage by plasma-sample interaction (see Fig. 4a (less fluence) and 4c (greater fluence, greater surface damage)). As the Zn is more volatile, it should be favored at high fluence and that does not happen. Similarly, the Mo that is an element with high melting and boiling point, presents no fractionation, *i.e.* volatility does not appear to be responsible. The Al, that has relatively low ionization potential, did not present fractionation. In conclusion, Zn and Cd were the only elements that showed fractionation as function of fluence, but without sufficient evidence to explain it by volatility or ionization

potentials.

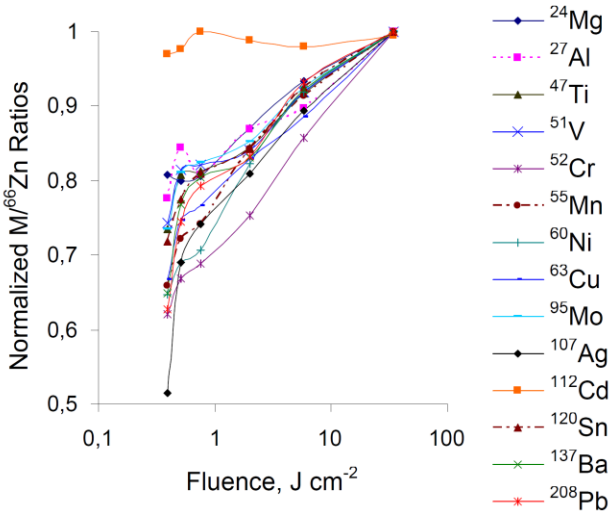

Figure 9: Normalized M (isotopes indicated) / ^{66}Zn ratios versus fluence (J cm^{-2}). Each point represents three 2 min 30 s runs average of acquisition signal at a scanning speed of 20 µm

It can be thought that the results of Fig. 9 may be influenced by mass load effect, because there is greater quantity of particles at low fluences (greater defocus and larger diameter) than at high fluences (see Fig. 8).

The ICP may be affected, decreasing its ionization temperature as a result of a large mass load, which can cause different ionization profiles for elements with different ionization potentials.

To evaluate this effect with crude oil sample, the analysis with different crater diameters while remained fixed the fluence was performed. Fig. 10 shows ^{63}Cu/^{66}Zn, ^{95}Mo/^{112}Cd, ^{27}Al/^{24}Mg and ^{60}Ni/^{63}Cu ratios which differ in ionization potential (expressed as $PI_{denominator}$ - $PI_{numerator}$) 1.68; 1.89; 1.66 y 0.09 eV respectively. It was observed that ratios tend to increase when mass load increases. This effect was more marked for the ^{95}Mo/^{112}Cd ratio, which has the largest difference in ionization potential. On the contrary ^{60}Ni/^{63}Cu ratio shows no significant change, since their PI not differ greatly.

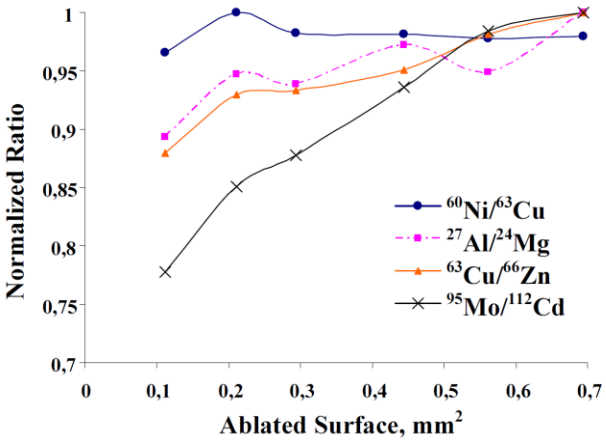

Figure 10: Normalized $^{63}Cu/^{66}Zn$, $^{95}Mo/^{112}Cd$, $^{27}Al/^{24}Mg$ and $^{60}Ni/^{63}Cu$ ratios versus crater surface. Each point represents three 2 min 30 s runs average of acquisition signal at a scanning speed of 20 µm

At higher mass load, the ICP diminishes its ionization temperature and those elements with high ionization potential are more affected which explains the results of Fig. 10.

If mass load had an effect on the results of Fig. 9, they had a decreasing trend (because the greater mass load is found in the low fluence analyse), confirming that the results are effects mainly produced by the ablation processes at different fluences and not by the processes occurring in the ICP.

CONCLUSIONS

Fractionation was observed as function of fluence, *i.e.* Zn and Cd signals were affected in different manner, respect to the other 13 elements studied, when fluence is increased. Elements with low ionization potential as Al or low volatility as Mo, showed no fractionation when fluence is varied. Therefore, there was insufficient evidence to explain the results in terms of the volatility and the ionization potential. Craters pictures are evidence that ablation mechanisms are changed at different fluence (see Fig. 4). They showed greater surface damage at higher fluence. It can be probably due to plasma-sample interaction. Also, differences among He and Ar ablation gases were observed. The best results, in terms of sensitivity and precision were obtained when He was used as ablation gas. Fractionation was also observed in the ICP. At higher mass load were disadvantaged those elements with high ionization potential due to the decreased of plasma ionization temperature. Conditions of increased sensitivity to the extra heavy crude oil were determined in the LA-ICP-MS system. It was found that they correspond mainly to a larger area of ablation (larger diameter and higher defocus level), high laser energy and high pulse frequency. Furthermore, an improvement in the stability of the signal was observed when a cyclonic chamber was used in the transport

system, this may promote the use of various devices in the transport system to improve analysis precision of related samples with high organic matter content. Under performed conditions, %RSD from 3 to 5% in the net signal of Cu, Zn, Ni and Mo and from 0.9 to 3.3% in the Ni/Mo and Cu/Zn ratios were found, respectively. The results of this study show the possibility of performing elemental determinations in extra heavy crude oil by ns-LA-ICP-MS. However, further experiments are needed for the purpose of increasing the sensitivity of the analytes, improve precision, reduce mass load effects and make the method robust to small matrix changes.

ACKNOWLEDGEMENTS

We thank PDVSA-INTEVEP S.A. for the financial support.

REFERENCES

1. Ricard E, Pécheyran C, Sanabria G, Prinzhofer A, Donard OFX, Direct analysis of trace elements in crude oils by high-repetition-rate femtosecond laser ablation coupled to ICPMS detection, Anal Bioanal Chem, 2011; 399:2153-2165.
2. Vorapalawut N, Pohl P, Bouyssiere B, Shiowatana J, Lobinski R, Multielement analysis of petroleum samples by laser ablation double focusing sector field inductively coupled plasma mass spectrometry (LA-ICP MS), J Anal At Spectrom, 2011; 26:618-622.
3. Heilmann J, Boulyga SF, Heumann KG, Development of an isotope dilution laser ablation ICP-MS method for multi-element determination in crude and fuel oil samples, J Anal At Spectrom, 2009; 24:385-390.
4. Herbert CG, Johnstone RAW, Mass Spectrometry Basics. CRC Press, New York, 2003.
5. Koch J, Gunther D, Laser Ablation ICP-MS. Encyclopedia of Spectroscopy and Spectrometry, 2nd edn, 2009;1262-1269.
6. Fernández B, Claverie F, Pécheyran C. Donard OFX, Direct analysis of solid samples by fs-LA-ICP-MS, Trends in Anal. Chem, 2007; 26:951-966.
7. Hergenröder R, Laser-generated aerosols in laser ablation for inductively coupled plasma spectrometry, Spectrochim Acta Part B, 2006; 61:284-300.
8. Hill SJ, Inductively Coupled Plasma Spectrometry and its Applications. Blackwell Publishing, Oxford, 2007.
9. Garcia CC, Lindner H, Von Bohlen A, Vadla C, Niemax K, Elemental fractionation and stoichiometric sampling in femtosecond laser ablation, J Anal At Spectrom, 2008; 23:470-478.
10. Miller JC, Hanglund RF, Laser Ablation and Desorption, Academic Press, San Diego, 1998.
11. Garcia CC, Lindner H, Niemax K, Laser ablation inductively coupled plasma mass spectrometry—current

shortcomings, practical suggestions for improving performance, and experiments to guide future development, J Anal At Spectrom, 2009; 24:14-26.

12. Bian Q, Garcia CC, Koch J, Niemax K, Non-matrix matched calibration of major and minor concentrations of Zn and Cu in brass, aluminium and silicate glass using NIR femtosecond laser ablation inductively coupled plasma mass spectrometry, J Anal At Spectrom, 2006; 21:187-191.
13. Koch J, Wälle M, Pisonero J, Günther D, Performance characteristics of ultra-violet femtosecond laser ablation inductively coupled plasma mass spectrometry at ~265 and ~200 nm, J Anal At Spectrom, 2006; 21:932-940.
14. Bian Q, Koch J, Lindner H, Berndt H, Hergenröder R, Niemax K, Non-matrix matched calibration using near-IR femtosecond laser ablation inductively coupled plasma optical emission spectrometry, J Anal At Spectrom, 2005; 20:736-740.
15. Glaus R, Kaegi R, Krumeich F, Günther D, Phenomenological studies on structure and elemental composition of nanosecond and femtosecond laser-generated aerosols with implications on laser ablation inductively coupled plasma mass spectrometry, Spectrochim Acta Part B, 2010; 65:812-822.
16. Kosler J, Wiedenbeck M, Wirth R, Hovorka J, Sylvester P, Míková J, Chemical and phase composition of particles produced by laser ablation of silicate glass and zircon—implications for elemental fractionation during ICP-MS analysis, J Anal At Spectrom, 2005; 20:402-409.
17. Wälle M, Koch J, Flamigni L, Heiroth S, Lippert T, Hartung W, Günther D, Detection efficiencies in nano- and femtosecond laser ablation inductively coupled plasma mass spectrometry, Spectrochim Acta Part B, 2009; 64:109-112.
18. Guillong M, Horn I, Günther D, A comparison of 266 nm, 213 nm and 193 nm produced from a single solid state Nd:YAG laser for laser ablation ICP-MS, J Anal At Spectrom, 2003; 18:1224-1230.
19. Jochum KP, Stoll B, Herwig K, Willbold M, Validation of LA-ICP-MS trace element analysis of geological glasses using a new solid-state 193 nm Nd:YAG laser and matrix-matched calibration, J Anal At Spectrom, 2007; 22:112-121.
20. Kroslakova I, Günther D, Elemental fractionation in laser ablation-inductively coupled plasma-mass spectrometry: evidence for mass load induced matrix effects in the ICP during ablation of a silicate glass, J Anal At Spectrom, 2007; 22:51-62.